# Behavior of the He II $3s, p, d-4s, p, d, f$ Line Complex in a Hollow Cathode Plasma*

FRED L. ROESLER AND J. E. MACK
*University of Wisconsin, Madison, Wisconsin*

(Received 23 September 1963; revised manuscript received 17 February 1964)

The fine structure of the He II $3s, p, d-4s, p, d, f$ line complex ($\sigma = 21\,335$ K, $\lambda = 4686$ Å) as observed in a hollow cathode cooled in liquid helium has been studied with a photoelectric double Fabry-Perot spectrometer. The traces show excellent resolution. Among the component lines: (1) The relative intensities tend, with increasing pressure in the discharge region, toward the calculated statistical intensities, and with decreasing pressure, not toward Bethe's dynamical intensities but in each case toward a dynamical intensity determined by the lifetime and rate of excitation of the initial state. (2) The measured relative positions are in good agreement with those calculated from quantum electrodynamics; small apparent discrepancies are believed to be associated with the excitation conditions. (3) The widths of the lines are appreciably greater than the widths of the He I lines at $\sigma = 21\,218$ K, the derived widths being 74 and 44 mK, respectively. (4) The positions are significantly shifted (~4 mK) due to a drift of the $He^+$ ions toward the cathode, and there is evidence that the lines of the neutral atoms are shifted (~1 mK) due to a motion of the emitters toward the anode.

## I. INTRODUCTION: PREDICTED LEVELS AND INTENSITIES

THE He II $3s, p, d-4s, p, d, f$ line complex (at 21 335 K, 4686 Å) has undergone a considerable amount of study throughout the development of the understanding of one-electron atoms. The fine structure of this complex was first partly resolved by Paschen[1,2] and interpreted with respect to Sommerfeld's theory, and later with respect to the Dirac theory, which led to the same energy levels. With the discovery of the anomaly found by Houston and Hsieh[3,4] and measured by Lamb and Retherford[5] in the hydrogen atomic spectrum, this transition took on new interest. Evidence of an upward shift in the $^2S_{1/2}$ levels involved in this transition was put forth by Mack and Austern,[6] and the measurements have since been gradually improved.[7–12] The current agreement between observation and prediction[13] with regard to the energy levels of one-electron atoms is generally excellent, especially for those term differences which it is possible to measure by microwave techniques. Although microwave measurements of the $3s-3p$ and $4s-4p$ term differences have not yet been successful,[14] it seems that, at least to the precision with which it is possible to measure term differences by optical spectroscopy, there can hardly be room for doubt as to the validity of the predictions of quantum electrodynamics.

On the other hand, almost every optical investigation of the hydrogen-like fine structure has revealed intensity anomalies. An anomaly in the $3s, p, d-4s, p, d, f$ complex was noticed by Austern,[15] first reported by Series,[11] and discussed somewhat further by Herzberg[12]; however, in no case up to now has apparatus suitable for precise intensity measurement been used.

In the present experiments a hollow cathode discharge and a photoelectric Fabry-Perot spectrometer were used to investigate the behavior of the complex as a function of pressure, temperature, current, potential difference, and geometry of the discharge region. The superior fine structure resolution achieved made it possible to do significant experiments on (1) the relative intensities of the lines, (2) their positions, (3) their widths, and (4) their shifts with a change in polarity of the source.

*The theoretical term values* for one-electron atomic spectra are given by quantum electrodynamics as

$$T_{nlj} = -\frac{Z^2 R_\infty}{n^2}\left(1-\frac{m}{M}\right)\left[1+\left(\frac{Z\alpha}{n}\right)^2\left(\frac{2n}{2j+1}-\frac{3}{4}\right)+\cdots\right] - \frac{Z^4\alpha^2 R_\infty m}{4n^4 M}+\Lambda(n,l,j)\,, \quad (1)$$

where $R_\infty$ is the Rydberg constant for infinite nuclear mass, $m$ and $M$ the mass of the electron and nucleus, respectively, $\alpha$ the fine structure constant, and $\Lambda(n,l,j)$ the quantum electrodynamic shift. In these expressions, only those terms which optical techniques are capable

* Supported by the National Science Foundation and by the Research Committee of the Graduate School of the University of Wisconsin from funds supplied by the Wisconsin Alumni Research Foundation.

[1] F. Paschen, Ann. Physik **50**, 901 (1916).
[2] F. Paschen, Ann. Physik **82**, 689 (1927).
[3] W. V. Houston and Y. M. Hsieh, Phys. Rev. **45**, 263 (1934).
[4] W. V. Houston, Phys. Rev. **51**, 446 (1937).
[5] W. E. Lamb, Jr. and R. C. Retherford, Phys. Rev. **72**, 241 (1947).
[6] J. E. Mack and N. Austern, Phys. Rev. **72**, 972 (1947).
[7] H. Kopfermann and W. Paul, Nature **162**, 33 (1948).
[8] H. Kopfermann, H. Kruger, and H. Ohlmann, Z. Physik **126**, 760 (1949).
[9] K. Murakawa, S. Suwa, and T. Kamei, Phys. Rev. **76**, 1721 (1949).
[10] J. G. Hirschberg and J. E. Mack, Phys. Rev. **77**, 745 (1950).
[11] G. W. Series, Proc. Roy. Soc. (London) **A226**, 377 (1954).
[12] G. Herzberg, Z. Physik **146**, 269 (1956).
[13] G. W. Series, *Spectrum of Atomic Hydrogen* (Oxford University Press, London, England, 1957).
[14] G. W. Series and W. N. Fox, J. Phys. Radium **19**, 850 (1958).
[15] N. Austern (private communication, 1947).

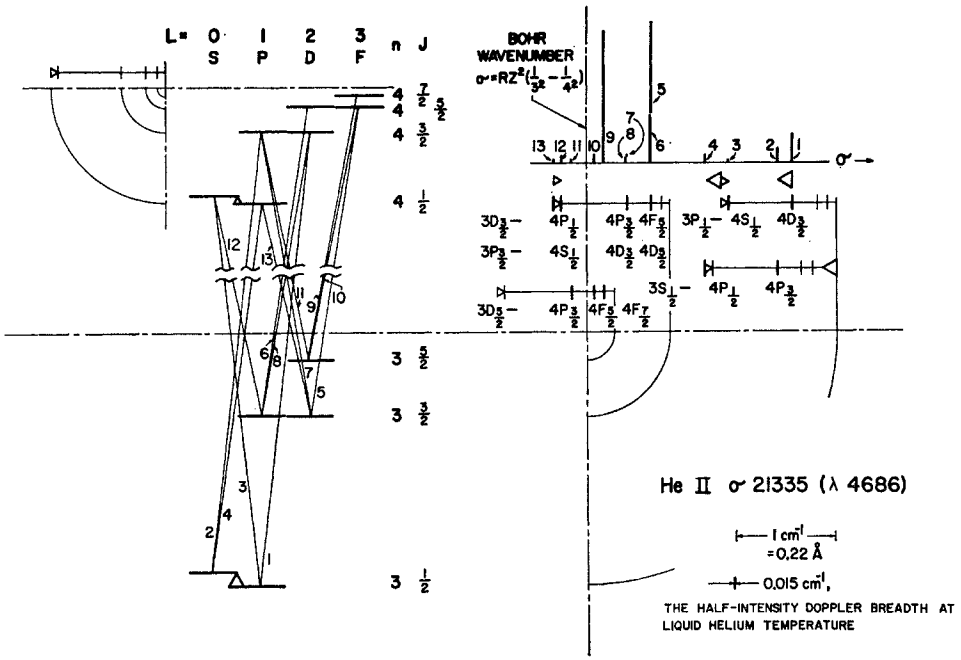


FIG. 1. The "Paschen Line" of ionized helium (actually the $3s, p, d-4s, p, d, f$ line complex). The dot-dash lines represent the Bohr terms and the horizontal full lines the calculated energy levels. The $3s\ ^2S_{1/2}$ and $4s\ ^2S_{1/2}$ quantum electrodynamical shifts are indicated by the large and small triangles, respectively. Shifts in other levels are indicated, but the scale is too small to show them quantitatively. The relative positions of the fine structure components were found by projecting the levels along horizontal axes as indicated by the curved lines and measuring off the $n=4$ pattern from each of the $n=3$ levels. The short, heavy vertical bars indicate the positions of the allowed lines; the heights of the vertical bars above these positions indicate the statistical relative intensities. The width of the bars in mK is shown as 15 mK, the Doppler half-intensity width the lines would have if the emitting ions were at the temperature of liquid helium.

of measuring are to be retained. $\Lambda(n,l,j)$ is then[16–19]

$$\Lambda(n,0,\tfrac{1}{2})=\frac{8Z^4\alpha^3}{n^3 3\pi}R_\infty\left(1-\frac{3m}{M}\right)\left\{-\ln\alpha^2 k_0(n,0)+\frac{19}{30}-\frac{3\times 0.328\alpha}{8\pi}+3\pi Z\alpha\left[\frac{427}{384}-\tfrac{1}{2}\ln 2\right]\right\},$$

or when $l\neq 0$,

$$\Lambda(n,l,j)=\frac{8Z^4\alpha^3}{n^3 3\pi}R_\infty\left(1-\frac{2m}{M}\right)\times\left[-\ln k_0(n,l)\pm\frac{3}{4}\frac{(1-0.328\alpha/\pi)}{(2j+1)(2l+1)}\right],$$

where the upper or lower sign is used according as $j=l\pm\frac{1}{2}$. The term $k_0(n,l)$ is the so-called average excitation energy, with the numerical values already computed[20] but here made dimensionless and expressed to enough digits for a precision of $10^{-9}R_\infty$ or 0.1 mK (1 K = 1 cm$^{-1}$) in level differences; $k_0(n,0)$ includes the factor $Z^2=4$ appropriate to He II and the values of $k_0(4,l)$ for $l>1$ are estimated.

$$k_0(3,0)=67.7,\quad k_0(3,1)=0.963,\quad k_0(3,2)=0.995,$$
$$k_0(4,0)=62.6,\quad k_0(4,1)=0.96,\quad k_0(4,2)=0.99,$$
$$k_0(4,3)=1.00.$$

Only the abundant isotope $He^4$, which is without hyperfine structure, need be considered as the intensities of the $He^3$ lines were completely negligible in the natural helium used in the experiment.

In Fig. 1, the left side shows the energy level diagram for $n=3$ and $n=4$, and the right side, the relative positions of the fine structure lines. The 13 lines have been assigned numbers in order from high to low wave number, which will frequently be used throughout the paper for ease of discussion.

Line intensities for one-electron spectra have been treated theoretically by Bethe and Salpeter.[21,22] The results important to this study are summarized here.

Neglecting for the moment the effects of electron

[16] N. H. Kroll and W. E. Lamb, Phys. Rev. **75**, 388 (1949).
[17] H. A. Bethe, L. M. Brown, and J. R. Stehn, Phys. Rev. **77**, 370 (1950).
[18] E. E. Salpeter, Phys. Rev. **89**, 92 (1963).
[19] R. Karplus, A. Klein, and J. Schwinger, Phys. Rev. **86**, 288 (1952).
[20] J. M. Harriman, Phys. Rev. **101**, 594 (1956).
[21] H. A. Bethe, in *Handbuch der Physik* edited, by H. Geiger and Karl Scheel (Julius Springer Verlag, Berlin, 1933), Vol. 24, p. 445.
[22] H. A. Bethe and E. E. Salpeter, *Quantum Mechanics of One- and Two-Electron Atoms* (Academic Press Inc., New York, 1957). Chap. IV, p. 248.

spin, and assuming that the electrons are distributed among the levels with a certain $n$ according to their statistical weights, i.e., that on the average there is one electron in each state $nlm$, we may write the intensity of the line $n'l'-nl$ as

$$J_{nl}^{n'l'}=(2l+1)h\nu_{nl,n'l'}A_{nl}^{n'l'}, \quad (2)$$

where $\nu$ is the frequency of the line and $A_{nl}^{n'l'}$ the dipole transition probability given by

$$A_{nl}^{n'l'}=\frac{4}{3}\frac{e^2\nu^3}{h}\left|\int\psi_{n'l'}^{*}r\psi_{nl}d\tau\right|^2.$$

Values of these so-called statistical intensities are tabulated in the middle column of Table I.

TABLE I. Computed intensity sums for He II $3s$, $p$, $d-4s$, $p$, $d$, $f$.

| | Statistical ($\times10^{-4}$ ergs/sec) | Bethe's dynamical ($\times10^{-4}$ ergs/sec) |
|---|---|---|
| $3s-4p$ | 6.16 | 0.472 |
| $3p-4s$ | 1.216 | 1.720 |
| $3p-4d$ | 23.68 | 5.36 |
| $3d-4p$ | 0.704 | 0.0540 |
| $3d-4f$ | 64.64 | 29.28 |

The intensities calculated from Eq. (2) are valid only if the excitation conditions produce a statistical distribution. With different excitation conditions a different set of intensities may well be observed. For example, if the excitation mechanism is such that on the average one electron per unit time is delivered to each state $nlm$ (Bethe's dynamical case[21,22]), then the number of electrons occupying that state is equal to the lifetime $t_{nl}$ of the state. The intensity of the line $n'l'-nl$ is then

$$[J_{nl}^{n'l'}]=J_{nl}^{n'l'}t_{nl}. \quad (3)$$

The intensities $[J_{nl}^{n'l'}]$ are listed in the last column of Table I and the lifetimes[12] $t_{nl}$ in Table II.

TABLE II. Computed lifetimes of the He II $n=4$ terms.

| | ($\times10^8$ sec) |
|---|---|
| $4s\ ^2S$ | 1.4154 |
| $4p\ ^2P$ | 0.07687 |
| $4d\ ^2D$ | 0.2258 |
| $4f\ ^2F$ | 0.4531 |

If one now takes the electron spin into account, the doublet sum rules together with the selection rules and the intensities for transitions $n'l'-nl$ determined from Eq. (2) or Eq. (3) allow the intensities of the fine structure components to be determined.[23] The calculated intensities of all lines allowed in the $3s$, $p$, $d-4s$, $p$, $d$, $f$ complex, relative to that of $3d\ ^2D_{5/2}-4f\ ^2F_{7/2}$ as 100, are listed in Table III for both the statistical and Bethe's dynamical assumptions.

TABLE III. Computed relative intensities, He II $3s$, $p$, $d-4s$, $p$, $d$, $f$, for two special cases.

| Line number | Transition 3–4 | Statistical | Bethe's dynamical |
|---|---|---|---|
| 1 | $^2P_{1/2}-^2D_{3/2}$ | 21.27 | 10.60 |
| 2 | $^2S_{1/2}-^2P_{3/2}$ | 11.12 | 1.89 |
| 3 | $^2P_{1/2}-^2S_{1/2}$ | 1.11 | 3.46 |
| 4 | $^2S_{1/2}-^2P_{1/2}$ | 5.56 | 0.94 |
| 5 | $^2D_{3/2}-^2F_{5/2}$ | 70.00 | 70.00 |
| 6 | $^2P_{3/2}-^2D_{5/2}$ | 38.28 | 19.08 |
| 7 | $^2D_{3/2}-^2P_{3/2}$ | 0.13 | 0.02 |
| 8 | $^2P_{3/2}-^2D_{3/2}$ | 4.25 | 2.11 |
| 9 | $^2D_{5/2}-^2F_{7/2}$ | 100.00 | 100.00 |
| 10 | $^2D_{5/2}-^2F_{5/2}$ | 5.00 | 5.00 |
| 11 | $^2D_{5/2}-^2P_{3/2}$ | 0.63 | 0.11 |
| 12 | $^2P_{3/2}-^2S_{1/2}$ | 2.22 | 6.93 |
| 13 | $^2D_{3/2}-^2P_{1/2}$ | 1.13 | 0.19 |

## II. LIGHT SOURCE

The hollow cathode was used by Paschen[1] and its basic properties investigated by Schüler.[24,25] Although relatively little progress seems to have been made since towards understanding the details of the atomic processes involved, the usefulness of the source in high-resolution spectroscopy is widely recognized.[26,27] The principal advantage of the hollow cathode is that it produces strong excitation in a relatively gentle plasma, where effects tending to broaden and shift spectral lines are generally small (but see Secs. IV and V, below). Schüler found that the voltage rose by almost its whole value (in his case, about 130 V) from the cathode wall to the edge of the plasma, which is separated from the wall by approximately the mean free path of an electron in the gas of the discharge region, but that within the plasma the fields were only on the order of 1 V/cm. With current densities $\approx10$ mA/cm$^2$ and pressure about 1 Torr, the breadth of the emitted lines is generally determined mainly by the Doppler temperature broadening, which can be reduced by cooling the cathode. Sources can be operated in liquid helium.[28,29]

Examples of the sources used in the present study are shown in Fig. 2. The excellent results obtained by the Bellevue group[29] prompted the adoption of their basic hollow cathode design for this study. Figure 2A shows the adaptation used in most of the experiments reported here. It is designed to take advantage of the possibility of convective circulation bringing cold gas

[23] See Ref. 22, p. 269.

[24] H. Schüler, Physik. Z. **22**, 264 (1921).
[25] H. Schüler, Z. Physik **35**, 323 (1926).
[26] S. Tolansky, *High Resolution Spectroscopy* (Pitman Publishing Corporation, New York, 1947).
[27] J. E. Mack and H. Arroe, J. Opt. Soc. Am. **40**, 386 (1950).
[28] J. G. Hirschberg, Phys. Rev. **99**, 1898 (1955).
[29] J. Brochard, R. Chabbal, H. Chantrel, and P. Jacquinot, J. Phys. Radium **18**, 596 (1957).

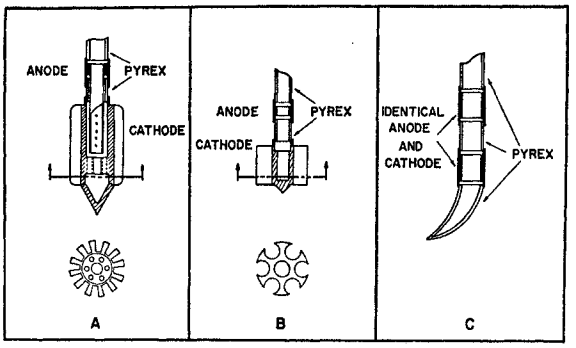


FIG. 2. Hollow cathodes used for exciting the He II spectrum at low temperatures: A—Bellevue type; B—simplified design; C—identical electrodes.

into the discharge region. The simplified design shown in Fig. 2B gave comparable results under the conditions of these experiments. (For a discussion of Fig. 2C, cf. Sec. V, below.)

The cathode and anode were machined from 99.9+% pure copper and joined to the Pyrex tube by a technique developed by Schroeder.[30] The ends of the copper pieces were machined with a ledge on a thin lip so that the Pyrex spacer or tube could be slip fitted inside the lip and butted against the ledge. The pieces to be joined were heated and coated with Bondmaster 702 epoxy cement which had been cast into sticks. The unit was assembled while the pieces were still warm enough so that the epoxy flowed readily and was cured at 150° for 4 h. Properly prepared units have withstood repeated operation in liquid $N_2$ and liquid He with no apparent deterioration

Figure 3 is a schematic drawing of the light source, Dewar, and vacuum system. The helium Dewar was surrounded by a jacket of liquid nitrogen. Current leads to the anode and cathode were 0.003-in. niobium wire, which is superconducting in the liquid helium bath but has a low thermal conductivity. By far the most important factor affecting the consumption of liquid helium was the power input of approximately one watt needed to excite the lines under study with sufficient intensity. Three liters of liquid helium transferred into the Dewar at the start of a run provided between 3 and 4 h of operation.

Sufficiently pure helium gas for filling the discharge tube was obtained from helium transferred from National Bureau of Mines tanks by two-step purification in out-gassed charcoal traps cooled with liquid nitrogen. When the source was operated in liquid helium, contamination by impurities was obviated by bending the inlet tube through the liquid helium before it joined the discharge tube. The glass wool trap prevented carbon dust from getting into the cathode region. The pressure in the tube was measured by a calibrated Pirani gauge.

[30] D. J. Schroeder, Ph.D. thesis, University of Wisconsin, 1960 (unpublished).

## III. SPECTROMETER

The Wisconsin Bellevue photoelectric Fabry–Perot spectrometer, employing two Fabry–Perot etalons in series with a grating monochromator, was used to study this structure. The principles of instruments of this type have been discussed elsewhere.[31–37] The present instrument differs from those previously described in several details, the most important of which are the simultaneous pressure scanning of the Fabry-Perot and the grating,[38] the interferometric calibration of the recorded spectra, and the synchronous pressure scanning of the double-etalon system by an improved technique developed for this study. A refinement of the latter detail has been described recently.[39] A paper describing the present instrument is in preparation.

For the study of the He II $3s, p, d-4s, p, d, f$ structure, the essential points are that (1) the Fabry-Perot spectrometer, when properly employed (and here proper employment implies the use of a double etalon system so long as the finesse remains less than about $10^2$), is about two orders of magnitude superior in luminosity to ordinary grating instruments operating at the resolution required in this study, and (2) the use of photoelectric detection affords linearity of response and relatively high quantum efficiency.

The importance of the first point arises because of

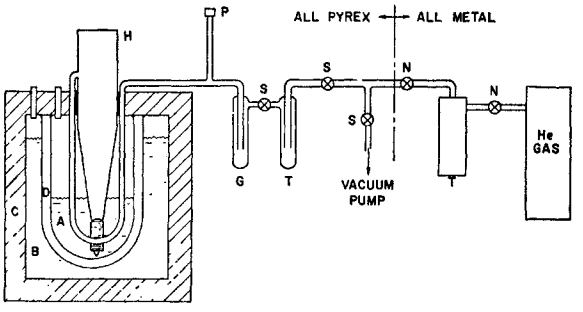


FIG. 3. The light source and vacuum system, schematic: A—liquid helium; B—liquid nitrogen; C—insulating box; D—vacuum Dewar; G—glass wool trap; H—hollow cathode tube; N—vacuum needle valves; P—Pirani gauge; S—stopcocks; T—charcoal traps.

[31] P. Jacquinot and C. Dufour, J. Rech. Centre Natl. Rech. Sci. Lab. Bellevue (Paris) **6**, 91 (1948).
[32] R. Chabbal, J. Rech. Centre Natl. Rech. Sci. Lab. Bellevue (Paris) **24**, 138 (1953); [English transl.: Document AERE Lib./Trans. 778, Harwell, England].
[33] P. Jacquinot, J. Opt. Soc. Am. **44**, 761 (1954).
[34] R. Chabbal, Rev. Optique **37**, 49 (1958).
[35] H. Chantrel, J. Rech. Centre Natl. Rech. Sci. Lab. Bellevue (Paris) **46**, 17 (1957).
[36] P. Jacquinot, Rept. Progr. Phys. **23**, 267 (1960).
[37] R. Chabbal and P. Jacquinot, Rev. Optique **40**, 157 (1961).
[38] J. G. Hirschberg and R. Kadesch, J. Opt. Soc. Am. **48**, 177 (1958).
[39] J. E. Mack, D. P. McNutt, F. L. Roesler, and R. Chabbal, Appl. Opt. **2**, 873 (1963).

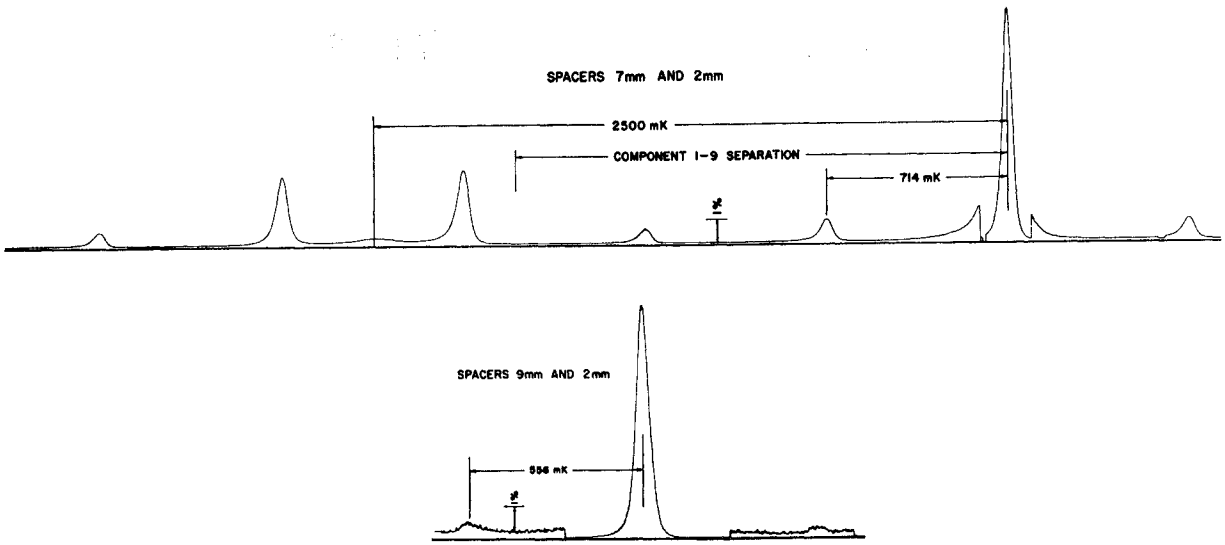


FIG. 4. Experimental double Fabry-Perot pass bands, $Hg^{198}$ 4916 Å. The discontinuous jumps of the tracing result from tenfold changes in the gain of the recorder and from zero light level checks.

the faintness of the He II line structure under study when it is excited under conditions which keep the linewidth small (cf. Fig. 5 below, where the lines of the He I multiplet $2p\ ^3P_{012}-4s\ ^3S_1$ at 21 218 K are seen to be more than 100 times stronger than those of He II $3s, p, d-4s, p, d, f$). The importance of the second point arises from the opportunity it offers for good relative intensity measurements.

Figure 4 shows test pass bands of the double Fabry-Perot system obtained with the 4916 Å line of $Hg^{198}$ from a microwave excited discharge. The upper recording on the figure shows the pattern of ghosts which arise from incompletely suppressed transmittance peaks of the two etalons. Usually considerably better suppression was attained, as shown by the lower trace of a small part of a pattern taken just before a run in liquid helium. Consideration must be given to the positions and strengths of these ghosts as well as to the desired resolution in choosing the ratio and magnitudes of the spacers. In the present work, spacers of 2 and 5 mm or 2 and 7 mm were used when the cathode was cooled in liquid nitrogen, and spacers of 2 and 9 mm when the cathode was cooled in liquid helium. In these cases, the resolution is commensurate with the component linewidth achieved under the excitation conditions, and no ghost of a strong line occurs with a weak line.

## IV. WIDTH OF THE ION LINES

When the hollow cathode is run in liquid helium, the lines of the He II $3s, p, d-4s, p, d, f$ complex are observed to be much wider than those of He I $2p\ ^3P_{0,1,2}-4s\ ^3S_1$ ($\sigma=21\ 218$ K, $\lambda=4713$ Å). The magnitude of the width difference is shown in Fig. 5, in which recordings of these two line complexes from a liquid helium cooled hollow cathode are superimposed. The two recordings are successive traces taken as near together in time as possible (about 20 min apart), at nearly the same rate, and under identical discharge conditions. On the assumption that the He I lines are broadened principally by the thermal Doppler effect, the temperature in the discharge region is found to be about 35°K. The apparent temperature derived from the width of the He II lines (corrected for instrumental width) is about 100°K.

The width of the lines was investigated at constant current over a change of nearly one order of magnitude in pressure (0.05 to 0.40 Torr). Within the experimental

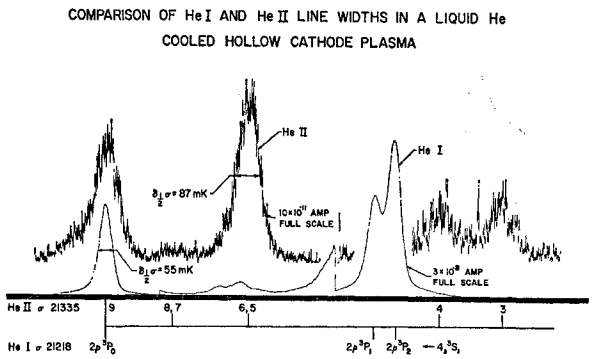


FIG. 5. Comparison of He I and He II linewidths in a liquid helium cooled hollow cathode plasma. The indicated widths must be corrected for the instrumental width to derive the true linewidth. In the interval between the He I $2p\ ^3P_{1,2}-4s\ ^3S_1$ blend and the He I $2p\ ^3P_0-4s\ ^3S_1$ line, the gain was increased from $3\times10^{-8}$ A to $3\times10^{-9}$ A full scale in order to show a ghost of the $2p\ ^3P_{1,2}-4s\ ^3S_1$ blend, whose intensity is approximately 0.006 times that of the parent structure. The gain for the $^3P_0-^3S_1$ line is $10\times10^{-9}$ A full scale. The gain of lines Nos. 3 and 4 of the He II structure is $3\times10^{-11}$ A full scale.

uncertainty, which is about $\pm 3$ mK for the strong lines, there is no change in width. If any change were to be inferred from the data, it would be a slight tendency for the width to increase as the pressure is decreased, but this is within the estimated uncertainty; the investigation shows that to a good approximation the broadening mechanism is independent of the proximity of neighboring atoms.

The following consideration shows that Stark effect can hardly be the cause. The usual approximate calculations applicable to the degenerate case, showing a linear effect, are, of course, inapplicable to the fully resolved spectrum. The position of $nS_{1/2}$ or $nP_{1/2}$ in a Stark field of magnitude $E$(V/cm) with respect to the field-free $nP_{1/2}$ level, as given by Bethe and Salpeter[40] (here modified to values in mK), is

$$\sigma-\sigma_0(np\,^2P_{1/2})=[\Lambda(n,0,\tfrac{1}{2})-\Lambda(n,1,\tfrac{1}{2})]/2 \pm\tfrac{1}{2}\{[\Lambda(n,0,\tfrac{1}{2})-\Lambda(n,1,\tfrac{1}{2})]^2 +18.20\times10^{-4}(n^2-1)(nE/Z)^2\}^{\frac{1}{2}}\text{ mK}, \quad (4)$$

where the (+) refers to the $S$ level and the (−) to the $P$ level. Thus, lines 3 and 4 are pushed farther apart as shown in Fig. 7, below, by the presence of an external electric field regardless of its origin. The magnitude of the increased separation is $4.5\times10^{-4}$ mK, 4.5 mK, and $3.3\times10^{3}$ mK for fields of 1, $10^2$, and $10^4$ V/cm. As a consequence, if the extra width of the ion lines is due to Stark effect, lines 3 and 4 ought to show a marked asymmetry and a separation far from the calculated value. Neither is observed. Similar arguments could be made for other lines.

A qualitative explanation of the greater width of the ion lines might be the following: The high-temperature electron gas in the plasma heats the ions sufficiently fast because of the strength of the Coulomb interaction between electrons and ions, to maintain the ion gas at a temperature higher than that of the relatively much more dense background gas of neutral atoms. Another possibility that might be investigated is the pumping of energy into the ions through plasma oscillations by a mechanism similar to that proposed[41] to explain the excessive width of ion lines observed in high-energy plasmas.

## V. DOPPLER SHIFT OF ION LINES

The concept of the ion gas as a separate species in the plasma is supported by the observed Doppler shift of the ion lines. The ion gas would be expected to move in the direction of the electric field with an average velocity equal to the drift velocity of $He^+$ ions in He.

A hollow-cathode tube (Fig. 2C) was designed with identical coaxial cylinders as electrodes. Either cylinder could be made the cathode. The direction of the field was away from the spectrometer in one case and toward the spectrometer in the other. A number of traces were made of both the strongest of the He II lines (i.e., line 9, $3d\,^2D_{5/2}-4f\,^2F_{7/2}$) and He I $2p\,^3P_0-4s\,^3S_1$, reversing the polarity between traces. The position of the lines relative to the reference fringe was measured, and a clear shift of the ion line was noted.

The observed shifts (called positive when they showed motion of the emitters in the direction of the field) were

$$\Delta\sigma\ (\text{He II } 3d\,^2D_{5/2}-4f\,^2F_{7/2})=(+7.4\pm1.4)\text{ mK},$$
$$\Delta\sigma\ (\text{He I } 2p\,^2P_0-4s\,^3S_1)=(-1.2\pm1.3)\text{ mK}.$$

Measured from the zero-field position the shift would have just half the above listed value.

The component of the average field along the axis of the discharge may be calculated upon the assumption that the shift of the ions is due to their drift velocity $v_d$ in the electric field $E$. Then

$$E=v_d/\mu=c\Delta\sigma/\mu\sigma=[0.5\pm0.1]\text{ V/cm}, \quad (5)$$

where $\mu$ is the mobility of helium ions in helium at the neutral gas temperature and pressure in the hollow cathode, and $c$ is the velocity of light. The value of $\mu$ was taken as $1.0\times10^4$ cm$^2$/V-sec.[42]

There seems also to be a real shift of the neutral helium line. A shift of this sort has been observed in the lines of krypton 86.[43] The Kr I shift is in the same direction as the He I shift, i.e., against the field. The ratio of the Kr I shift to the He I shift is very roughly in the inverse ratio of the masses of the atoms: the mass ratio is 21.5 while the ratio of the shifts is about 1:10. This is consistent with the explanation given by Engelhard[44] that the Doppler shift of the neutral atomic line is caused by momentum transfer from electrons which drift opposite the field direction.

The importance of this drift shift in the determination of wavenumbers deserves emphasis. Evidently, measurements taken with the field direction alternately toward and away from the observer ought to be averaged.

## VI. RELATIVE LINE POSITIONS

Figure 6 shows a recording of the He II $3s$, $p$, $d-4s$, $p$, $d$, $f$ complex from a liquid helium cooled hollow cathode and part of its calibration chart. The superior resolution and precise calibration which were achieved on a number of such recordings allowed good measurements to be made on all the well resolved lines. Attempts were also made to decompose the unresolved or partly resolved structures except for the very close blends 5, 6 and 7, 8.

The effect of blending on the position of each line

[40] See Ref. 22, p. 240.
[41] J. G. Hirschberg and R. W. Paladino, Phys. Fluids **5**, 48 (1962).
[42] M. A. Biondi and L. M. Chanin, Phys. Rev. **94**, 910 (1954).
[43] C. F. Bruce and M. R. Hill, Australian J. Phys. **14**, 64 (1961).
[44] E. Engelhard, Proces-Verbaux des Seances du Com. Int. Poids Mes. **26B**, M58 (1957).

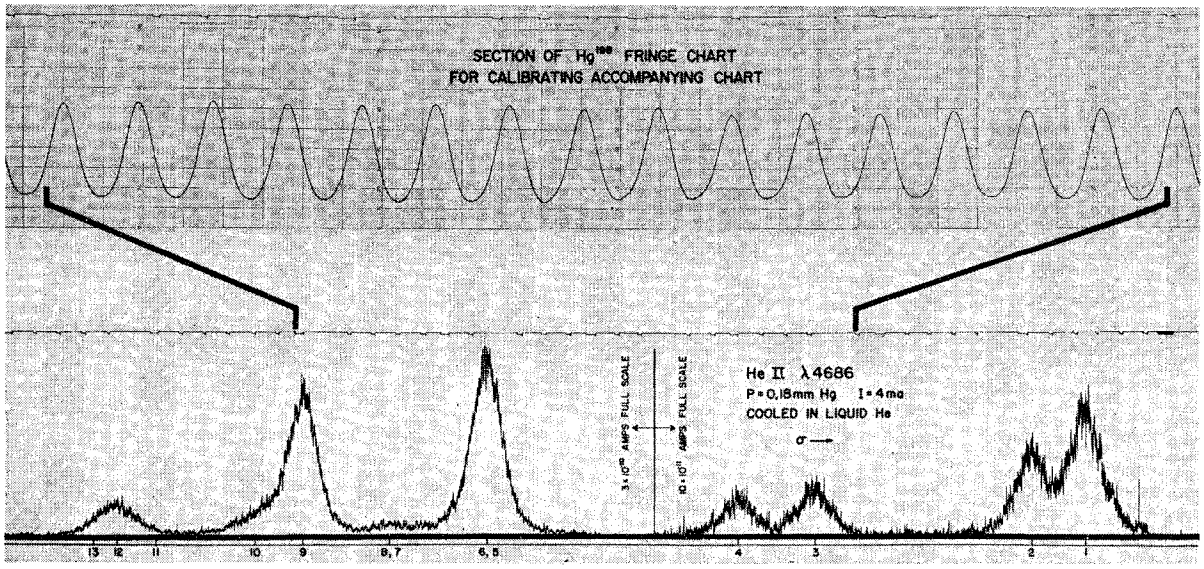


FIG. 6. The He II $3s, p, d-4s, p, d, f$ line complex observed in a liquid helium cooled hollow cathode. The calibration fringe chart is related to the spectrum chart through the coded intercalibration marks at the top of each chart. The heavy lines between the charts indicate the portion of the spectrum to which the reproduced portion of the fringe chart applies.

was considered. It was assumed that the lines would all have the same recorded profile if they were unblended. A standard profile was determined from the strong blend 5, 6, neglecting the small separation between 5 and 6 and subtracting the effect of components 7 and 8 on the red wing. An asymmetry, probably instrumental, was observed in the wings of the profile; such an asymmetry is evident in Fig. 4, above. This profile was applied to the various blends and the estimated heights and positions of the lines adjusted by successive approximations until their sum satisfactorily matched the recorded spectrogram.

When a satisfactory fit had been achieved, the center of each line was measured with respect to the reference fringes, and its separation in mK from line 9 (arbitrarily chosen as the reference point) computed. These separations are listed in Table IV and compared with the theoretical separations calculated from Eq. (1); but in order to calculate the terms to the nearest 0.1 mK it was necessary, in the case of the $j=\frac{1}{2}$ levels, to carry one more term in the series approximation than appears in Eq. (1). Table V, the rectangular array, shows the Dirac value and the modern theoretical value of each level and the observed minus the theoretical wave number of each line.

Figure 7 compares the positions of lines 1, 2, 3, and 4 measured in this study and the measurements of Series[11] and Herzberg[12] with the calculated positions. Also shown are calculated Stark shifts of the lines as functions of the electric field. Although this structure has been measured by a number of others, by far the best resolution has been achieved in these studies. The work reported by Series and by Herzberg was photographic: the former done with a double Fabry-Perot and the latter with a large grating instrument.

With regard to the present relative measurements, lines 1 and 3 agree with the calculated values, while both lines 2 and 4 disagree with the calculated values by about the same amount and in the same direction. If the measurements were taken as accurately representing the energy levels of a completely unperturbed atom, then one would have to infer from them a downward shift of the $3s\ ^2S_{1/2}$ level by about 6.5 mK from

TABLE IV. He II $3s, p, d-4s, p, d, f$ line positions relative to No. 9 ($3d\ ^2D_{5/2}-4f\ ^2F_{7/2}$), expressed in mK ($10^{-3}$ cm$^{-1}$).

| Line | Observed, 8 mm cathode | Observed, 12 mm cathode | Observed, all data | Uncertainty[a] | Theory | Obs.-theor. |
|---|---|---|---|---|---|---|
| 1 | 1947.6 | 1954.4 | 1948.2 | ±3 | 1945.2 | +3.0 |
| 2 | 1813.1 | 1813.4 | 1813.2 | ±3 | 1806.9 | +6.3 |
| 3 | 1275.4 | 1274.9 | 1275.2 | ±4 | 1273.4 | +1.8 |
| 4 | 1081.4 | 1081.1 | 1081.3 | ±3 | 1074.8 | +6.5 |
| 5 | | | | | 456.4 | |
| | 456.8 | 454.6 | 456.3 | ±1 | 455.5[b] | +0.8 |
| 6 | | | | | 453.8 | |
| 7 | | | | | 214.0 | |
| | 219 | 213 | 217 | ±5 | 210.0[b] | +7 |
| 8 | | | | | 209.8 | |
| 9 | 0 | 0 | 0 | ±3 | 0 | ... |
| 10 | −121 | −122 | −121 | ±4 | −122.0 | +1 |
| 11 | ... | ... | −354[c] | ... | −364.4 | +10 |
| 12 | −462 | −464 | −462 | ±3 | −462.0 | 0 |
| 13 | ... | ... | −504[c] | ... | −518.1 | +14 |

[a] Subjectively estimated probable error. The uncertainty in No. 9 is with respect to reference fringes and may reflect a change in Doppler shift with pressure; for other lines, the uncertainty is expressed with respect to No. 9 taken as exact.

[b] Measurement of blended components is compared with the center of gravity of the blend, calculated with statistical relative intensities.

[c] Observed positions for Nos. 11 and 13 are read from points $C_2$ of Fig. 8, below, but no attempt is made to estimate the uncertainty.

TABLE V. Observed minus theoretical line positions for He II $3s, p, d-4s, p, d, f$ lines relative to No. 9 ($3d\,^2D_{5/2}-4f\,^2F_{7/2}$, theoretical value, 21 335.0822 K). Levels are listed in K (1K=1 $cm^{-1}$), discrepancies in mK.

| Level | Dirac<br>q.e.d. corr<br>theory[a] | $3s\,^2S_{1/2}$<br>390 140.8027<br>+0.1377<br>390 140.9404 | $3d\,^2D_{3/2}$<br>390 142.5341<br>−0.0008<br>390 142.5332 | $3d\,^2D_{5/2}$<br>390 143.1111<br>+0.0005<br>390 143.1116 | $4s\,^2S_{1/2}$<br>411 477.0981<br>+0.0583<br>411 477.1563 | $4d\,^2D_{3/2}$<br>411 477.8285<br>−0.0003<br>411 477.8282 | $4d\,^2D_{5/2}$<br>411 478.0720<br>+0.0002<br>411 478.0722 |
|---|---|---|---|---|---|---|---|
| $3p\,^2P_{1/2}$ | 390 140.8027<br>−0.0019<br>390 140.8008 | | | | No. 3<br>+1.8±4 | No. 1<br>+3.0±3 | |
| $3p\,^2P_{3/2}$ | 390 142.5341<br>+0.0021<br>390 142.5362 | | | | No. 12<br>0±3 | No. 8<br>bl[b]+7 | No. 6<br>bl[b]+0.8 |
| $4p\,^2P_{1/2}$ | 411 477.0981<br>−0.0008<br>411 477.0973 | No. 4<br>+6.5±3 | No. 13<br>+14[c] | | | | |
| $4p\,^2P_{3/2}$ | 411 477.8285<br>+0.0009<br>411 477.8294 | No. 2<br>+6.3±3 | No. 7<br>bl[b]+7±5 | No. 11<br>+10[c] | | | |
| $4f\,^2F_{5/2}$ | 411 478.0720<br>−0.0002<br>411 478.0718 | | No. 5<br>bl[b]+0.8 | No. 10<br>+1±4 | | | |
| $4f\,^2F_{7/2}$ | 411 478.1937<br>+0.0001<br>411 478.1938 | | | No. 9<br>(ref. pt.) | | | |

[a] Values for the constants used in arriving at the theoretical positions are $\alpha^{-1}=137.0388$ exactly and $R(He^4)=109\,722.26733$ K computed from $m(He^4)$, $m_e$, and $R_\infty$ values taken to be exact: $m(He^4)$ from Everling, König, Mattauch, and Wapstra, Nucl. Phys. **15**, 342 (1960); $m_e$ and $R_\infty$ from a recommendation of the NAS–NRC committee on fundamental constants as listed in the Nat. Bur. Stds. (U.S.), Tech. News Bull. **47**, 175 (1963). Calculations were carried to more places than shown; apparent discrepancies in the last place shown arise from rounding to best final values.

[b] bl means, part of a blended pair; see Table IV, note b.

[c] The data shown for lines Nos. 11 and 13 are from the special procedure outlined at the end of Sec. VI and illustrated in Fig. 8, below.

the value calculated from quantum electrodynamics, or about 5% of the whole quantum-dynamical $3s$ shift of 138 mK. But in view of the success of the theory in accurately predicting Lamb shifts in $He^+$ measured by microwave techniques[45] it would be surprising if such a discrepancy actually existed. The whole problem of this differential shift will be discussed in another paper,[46] but can be outlined here. In a search for the cause of any such apparent shift the most likely contributions may be grouped into two general categories: false ones associated with the instrumental technique, and true ones associated with the environment of the emitting ions in the discharge tube.

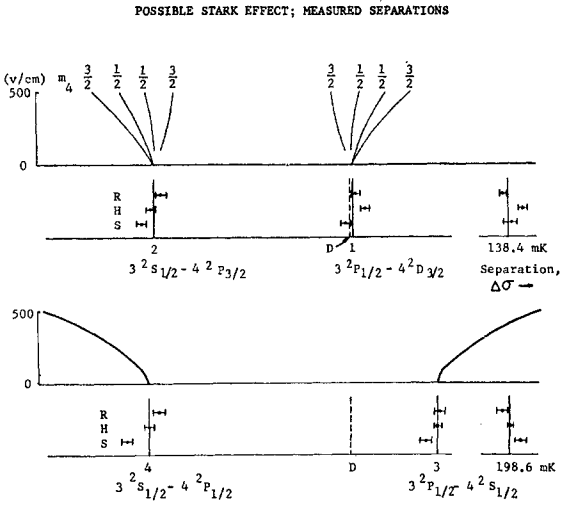


FIG. 7. Computed effect of an electric field on lines 1, 2, 3, 4, and measurements of the same lines by various authors: S=Series (Ref. 11), H=Herzberg (Ref. 12), R=present study. Upper half, lines 1 and 2; lower half, lines 3 and 4. The upper part of each half is a Stark effect plot showing the computed line positions (abscissas) as functions of the electric field **E** (V/cm). The curves that do not extend to **E**=0 are for line components whose intensities vanish at low fields. The lower part of each half shows the measured positions relative to line 9, and on the right, the measured separations. The numbers in mK are calculated zero-field separations. D denotes the Dirac position. Uncertainties shown for H and R are estimates of the probable error; for S, four times the probable error.

Within the former category, the uncertainty in the red wing of the recorded line profiles on which lines 2 and 4 lie might cause a shift of as much as 2 mK, but hardly more. Furthermore, the possibility of contamination from stray lines is present, especially in the case of pure Fabry-Perot spectroscopy, where an incompletely suppressed transmittance peak may mix a line from well outside the structure under study into the spectrographic record. Of particular concern in this respect are a band of the first negative system of $N_2^+$ with its head at 4709 Å, which has several components crossing the He II $3s, p, d-4s, p, d, f$ complex, and a $He_2$ band just to the violet of the complex. A careful search was made for stray lines, and with the instrument as finally adjusted for this study, none was detected.

[45] R. Novick, E. Lipworth, and P. E. Yergin, Phys. Rev. **100**, 1153 (1955).

[46] F. L. Roesler and Linda DeNoyer, Phys. Rev. Letters **12**, 396 (1964).

In the category of true atomic effects, several can be mentioned. Since the mechanism which gives the ion lines their excessive width is not completely understood, one cannot eliminate the possibility that the broadening mechanism impresses a shift on certain levels. Neither can one eliminate the possibility that the widths and shapes of the component lines differ somewhat among themselves, causing a systematic error to be introduced if a standard profile is applied to the analysis of the structure. There is some evidence for the latter, although the low signal-to-noise ratio makes determination of the widths and profiles of the weak components quite inaccurate. But the effect can be satisfactorily accounted for as a differential Doppler shift of the ion lines. The upper term of the shifted lines 2 and 4 is $4p\,^2P$. If, perhaps on account of being in an accelerating field for a shorter time, ions in $P$ states drifted sufficiently more slowly than those in $S$, $D$, or $F$ states, the observed results would be qualitatively obtained. The magnitude of the Doppler shift observed for line 9 is of the same order as the observed discrepancy in the relative positions of lines 2 and 4. The results of Series[11] as shown in Fig. 7 are consistent with this possibility. Series' measurements were made with the field in the discharge region directed towards the observer, while the results of the present study were obtained with the field directed away from the observer. Therefore, under the assumption of a differential drift, the shifts observed by Series would be expected to be about the same magnitude as the present shifts, but oppositely directed. Taking into account the discrepancy of about 6 mK between the measurements of Series and the other observations in the position of component 9, the expectation is seen to be fulfilled. The hollow cathode used by Herzberg offered the possibility of looking with the field in either direction.

The resolution in the measurements of Series and Herzberg was appreciably lower than that obtained in the present study, and consequently their measurements of components 1 and 2 are subject to considerable systematic error from the method of decomposition used. However, their resolution was sufficient to obtain measurements of the more widely spaced components 3 and 4 to an accuracy comparable with the present ones. Series was led to postulate a downward shift of the $4p\,^2P_{1/2}$ level from the calculated value because his measurement of the separation of 3 and 4 was greater than calculated by more than his estimate of error. Neither Herzberg's nor our measurements show such a shift.

An analysis of lines 11, 12, and 13 was hampered by lack of resolution. Since lines 11 and 13 are much weaker than line 12, the position of the peak of the blend is shifted only slightly by their presence from the position of 12. Therefore, in the initial decomposition of the blend, weak components were assumed at the positions deduced by means of the combination principle from measurements of other lines. Using the experimental profile, the position of 12 and the intensities of all three components were adjusted to fit the recording. The position and intensity of 12 were then measured.

When the position of line 12 and the 2:1 multiplet intensity ratio between 12 and 3 had been satisfactorily verified, 12 was subtracted from the blend, using the calculated position and twice the intensity of the relatively unblended line 3, the other member of its doublet. The residuals of many such operations performed on

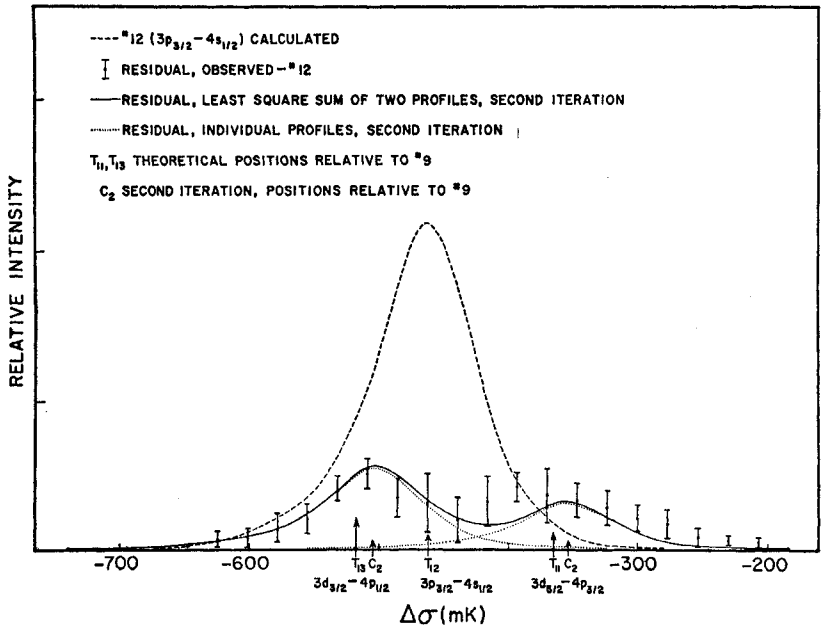


FIG. 8. Decomposition of components 11, 12, and 13.

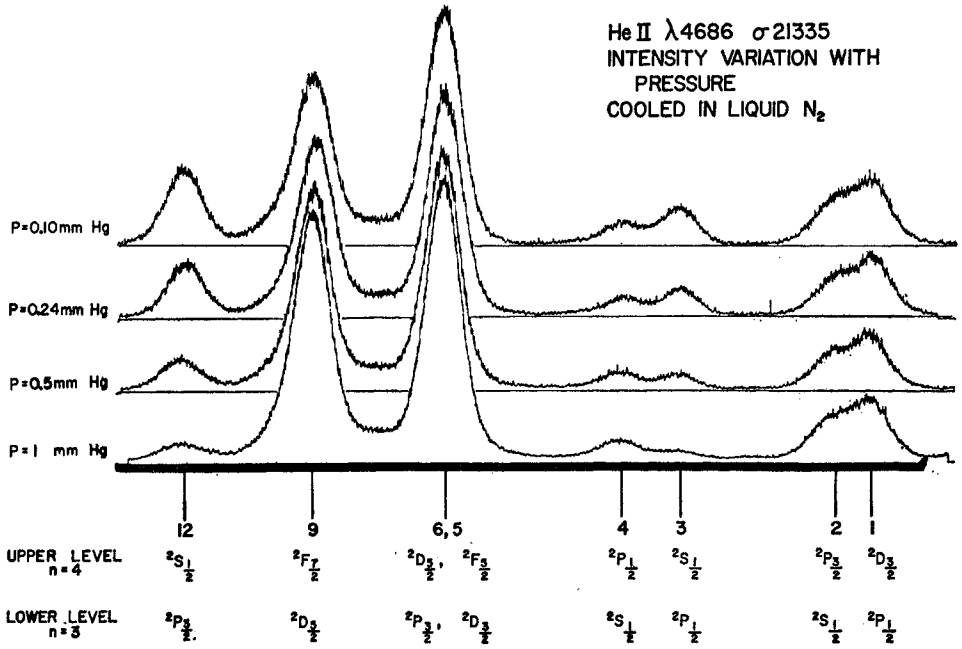


FIG. 9. Superposition of traces showing intensity variation with pressure in a liquid nitrogen cooled hollow cathode plasma. The current was 10 mA in each case. The gain for each trace was adjusted to keep the height of the blend Nos. 6, 5 roughly constant.

the recordings were averaged, using for normalization the intensity of line 4, which, like 11 and 13, has an upper $P$ level. A least-squares approximation using the experimental profile was used to place two components $C_2$ with the intensity ratio 9:5 with respect to the measured points. As can be seen from Fig. 8, the positions are in reasonable agreement with the calculated positions $T_{11}$ and $T_{13}$, though the agreement may be largely fortuitous; the deduced intensity of these components is too great by a factor about 2. When the cathode was operated in the higher pressure range where, according to Sec. VII, the relative intensities of lines 11, 12, and 13 ought to be most favorable for decomposition, there was a clear inconsistency with the calculated structure. In the higher pressure ranges the intensity of the band lines is relatively high compared to the He II intensity, and the possibility of contamination from a band line underlying the 11, 12, 13 structure seems strong. An unsuccessful search was made for lines lying away from the He II structure which might be mixed in by an etalon ghost.

## VII. RELATIVE LINE INTENSITIES

Figure 9 shows a superposition of a series of traces of the He II $3s, p, d-4s, p, d, f$ complex excited in a hollow cathode cooled by liquid nitrogen, with the pressure changed between traces, other variables being held constant. The most striking feature in this figure is the large variation in intensity shown by lines 3 and 12. This variation, along with less obvious variations in other lines, has been studied as a function of hollow cathode pressure, temperature, current, voltage, and diameter, not all of which are independent.

The intensities of all the lines which could be satisfactorily treated were measured relative to line 9 ($3d\,^2D_{5/2}-4f\,^2F_{7/2}$) as 100. Line 9 was chosen as the reference line because it is a single strong line with no very close blends. In making these measurements, due consideration was given, with the aid of a standard profile arrived at as explained in the previous section, to the blending of components.

### A. Pressure Variations

The general behavior of each measurable line is shown as a function of pressure in a liquid $N_2$ cooled hollow cathode (Fig. 10) and in a liquid helium cooled hollow cathode (Fig. 11). In both cases it can be seen that all the other lines increase in intensity relative to 9 as the pressure decreases, and that as the pressure increases the relative intensities approach the calculated statistical intensities (see Sec. I) indicated by the height of the vertical bar at each line position.

Figure 12 shows the ratio of the observed intensity $I_o$ to the calculated statistical intensity $I_s$ as a function of the pressure for several of the lines. If the relative intensities are statistical, then $I_o/I_s=1$. Within the experimental uncertainty, all the ordinates are seen to approach unity as the pressure increases. With increasing pressure, the uncertainty (not shown) becomes rather large because of the rapid decrease in the overall intensity of the He II complex; moreover, the danger of confusion from $He_2$ band lines within the observed structure increases, as nearby band lines are observed to become very strong with increasing pressure.

Thus, this study shows that within the limits of accuracy the calculated statistical intensities are valid whenever the pressure is high enough.

Figure 13 shows the observed intensity divided by

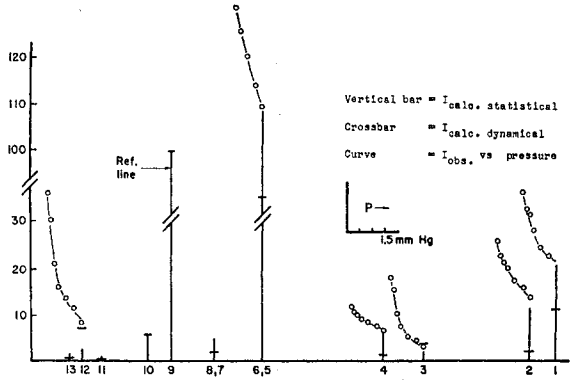


FIG. 10. Intensity variation of the He II $3s, p, d-4s, p, d, f$ line complex in a liquid nitrogen cooled hollow cathode. The height of the vertical bar is proportional to the calculated statistical intensity and the ordinate of the crossbar, to Bethe's dynamical intensity. The heights of the very close blends 5, 6 and 7, 8 have been added. Accompanying each component for which measurements were possible is a curve showing the observed intensity versus pressure; the pressure for each point may be found by adjusting the abscissa scale (insert) to read 1.5 Torr at each vertical bar.

the calculated Bethe dynamical intensity $I_d$ for the lines used for Fig. 12. $I_o/I_d$ would approach unity as the pressure approaches zero if Bethe's assumption used in Sec. I to calculate the dynamical intensities were valid. Clearly, this assumption was not correct for the actual excitation mechanism in the hollow cathode, for it failed to take into account the differences in the rates of excitation of the different levels.

It is possible, without going into the details of the processes involved, to derive a simple expression that roughly describes the way in which the relative intensities change with pressure.

Let $N_i$ represent the number of atoms in the $i$th excited level. In the absence of collisions with other atoms the rate at which atoms are excited to level $i$ is $Q_i$; atoms decay from this level at a rate $N_i/t_i$, where $t_i$ is the lifetime of the level. Let the mean time between collisions be called $t_c$; then the finite pressure in the discharge region causes atoms to collide at a rate $1/t_c$. If it is assumed that the only effect of the collisions is to rearrange the atoms among the set of levels $\{k\}$ which have nearly the same energy as level $i$, then

$$dN_i/dt=Q_i-N_i/t_i-(N_i/t_c)A+B/t_c, \qquad (6)$$

where $AN_i/t_c$ is the number lost from level $i$ due to collisions and $B/t_c$ is the number gained by level $i$ due to collisions of atoms in other levels of $\{k\}$. Then at equilibrium,

$$N_i=(Q_it_i+Bt_i/t_c)(1+At_i/t_c)^{-1}. \qquad (7)$$

If it is assumed that the terms $A$ and $B$ are the same for all levels of $\{k\}$, the population of the $i$th level relative to a reference level $r$ is

$$R_i=\frac{N_i}{N_r}=\frac{(Q_it_i+Bt_i/t_c)(1+At_r/t_c)}{(Q_rt_r+Bt_r/t_c)(1+At_i/t_c)}, \qquad (8)$$

which is the factor by which the relative statistical intensities ought to be multiplied to account for the non-statistical population distribution of the levels. For high pressures, $1/t_c$ becomes very large and $R_i \to 1$, so that statistical intensities are realized. At low pressures, $1/t_c \to 0$, so that $R_i \to Q_it_i/Q_rt_r$, the dynamical distribution, which is just Bethe's dynamical distribution adjusted for the different rates of excitation for the levels. Although Eq. (8) gives the limiting distributions, it does not give a good fit to the data when $A$ and $B$ are taken as constants.

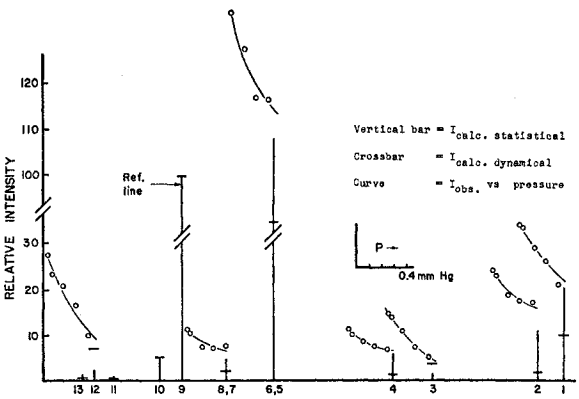


FIG. 11. Intensity variation of the He II $3s, p, d-4s, p, d, f$ line complex in a liquid helium cooled hollow cathode. Pressure dependence is shown as in Fig. 10; the pressure for each point may be found by adjusting the abscissa scale (insert) to read 0.37 Torr at each vertical bar.

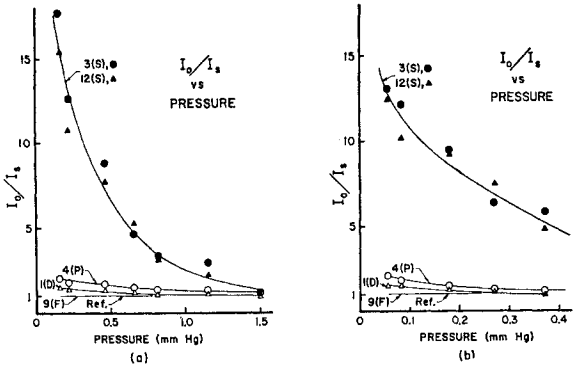


FIG. 12. Ratio of the observed intensity $I_o$ to the statistical intensity $I_s$ as a function of pressure for some of the lines of the He II $3s, p, d-4s, p, d, f$ complex observed from a hollow cathode cooled in (a) liquid nitrogen, (b) liquid helium. The $l$ value of the upper ($n=4$) level is given in parentheses.

## B. Intensities Within a Multiplet

It can be seen from Figs. 12 and 13 that the curves for lines 12 and 3 are essentially the same, as are the curves for lines 2 and 4. Lines 12 and 3 are the transitions $3p\ ^2P_{3/2,1/2}-4s\ ^2S_{1/2}$ and lines 2 and 4 the transitions $3s\ ^2S_{1/2}-4p\ ^2P_{3/2,1/2}$, respectively. The congruence

of the two curves in each case verifies the calculated intensity ratio of 2:1 and gives an indication of the reliability of the intensity measurements. The upper level for component 2, $4p\,^2P_{3/2}$, is almost degenerate with $4d\,^2D_{3/2}$, actually lying within its natural width (see Secs. I and VI) and one might expect $4p\,^2P_{3/2}$ and $4d\,^2D_{3/2}$ to be mixed by small external fields, causing a departure from the multiplet intensity ratio; but Bethe and Salpeter[47] have shown theoretically that even in the absence of a Lamb shift, these levels are not expected to be mixed unless there is a field of sufficient strength to cause the levels to split by an amount comparable with their natural widths. The required field can be shown to be of the order of 10 V/cm. This null result may be taken as further evidence of the absence of appreciable Stark effect in the center of a hollow cathode plasma.

The 2:1 intensity ratio of lines 2 and 4, furthermore, shows that the relative rates of excitation for the levels depend only on the $l$ values of the levels; were there a $j$ dependence, there would be a departure from this ratio as the pressure decreased.

The intensity ratios of lines 12 to 3 and 4 to 2 are the only multiplet intensity ratios that can be measured directly with reasonable accuracy. However, the ratio of line 1 to line 6, which is closely blended with 5, may be indirectly calculated. The theoretical ratio of line 9 to line 5 is 20:14, which, since line 9 has intensity 100 by definition, means that line 5 has intensity 70. Therefore, the subtraction of 70 from the measured intensity of the 5, 6 blend gives the intensity of 6. The ratio of lines 6 and 1 thus indirectly observed is 1.9, which is taken as verification of the predicted ratio 9:5 or 1.80 within the experimental accuracy. The intensity ratios for the multiplets which could be significantly measured are listed in Table VI.

TABLE VI. Observed intensity ratios within multiplets. (Uncertainties are estimates of the probable error.)

| Line numbers, ratio | Observed (all data) | Predicted |
|---|---|---|
| 12:3 | 2.0 ±0.1 | 2.00 |
| 2:4 | 2.06±0.1 | 2.00 |
| 6:1 | 1.9 ±0.2 | 1.80 |

## C. Relative Rates of Excitation

Extrapolation of the curves in Fig. 13 to zero pressure yields the ratio of the rate of excitation of the plotted initial level to that of the reference level. This is seen to be greatest for the $P$ levels (lines 2 and 4) followed by the $S$, $D$, and $F$ levels in that order. Upon the assumption that the excitation is principally electron excitation from the ground state of the ion, the rate of excitation is seen to depend upon the cross section for

[47] See Ref. 22, p. 290.

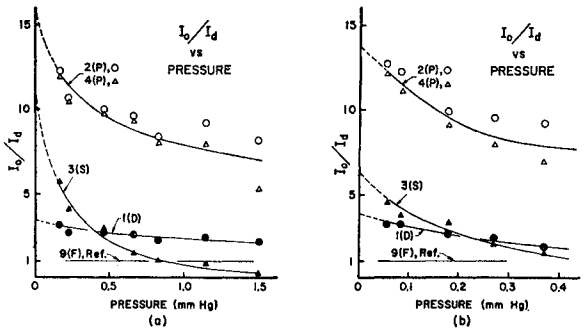


FIG. 13. Ratio of the observed intensity $I_o$ to Bethe's dynamical intensity $I_d$ as a function of pressure for some of the lines of the He II $3s, p, d-4s, p, d, f$ complex observed from a hollow cathode cooled in (a) liquid nitrogen, (b) liquid helium. The $l$ value of the upper ($n=4$) level is given in parentheses.

that process and upon the electron energy distribution. Cross section calculations for this process have not been carried out for the $n=4$ levels of $He^+$; however, corresponding cross sections for the excitation of the $n=4$ levels of atomic hydrogen have been computed and are tabulated by Massey and Burhop.[48] If the cross sections for $He^+$ have approximately the same relative values, there is qualitative agreement between the observations and the calculations, which show the greatest excitation for $P$ states, followed by $S$, $D$, and $F$ in that order. The ratios for the calculated values are roughly $S:P:D:F=1.00:7.6:0.25:0.003$, while the observed ratios as determined from Fig. 13 are $S:P:D:F=1.00:1.35:0.35:0.08$, where the value for the $S$ level has been arbitrarily set equal to 1. The rather large differences presumably arise because the excitation of the $n=4$ levels can be accomplished by a number of other processes of varying importance.

The relative rates of excitation of the various terms can be studied empirically by plotting $\log(I_o-I_s)/I_d$ versus pressure as shown in Fig. 14. In this case, the points at lower pressure fall on a straight line whose intercept on the ordinate is $\log(Q_i/Q_f-I_s/I_d)$, where $Q_i/Q_f$ is the rate of excitation of term $i$ relative to the reference term $f$. Relative rates of excitation determined in this way are shown in Table VII.

TABLE VII. Rates of excitation of the $n=4$ terms relative to the $4f$ term. ($C$=liquid coolant, $D$=cathode diameter in mm, $I$=current in mA.)

| Excitation conditions | | | Relative rates of excitation | | | |
|---|---|---|---|---|---|---|
| $C$ | $D$ | $I$ | $4s$ | $4p$ | $4d$ | $4f$ |
| $N_2$ | 8 | 10 | 9.3 | 14 | 4.5 | 1.00 |
| $N_2$ | 12.7 | 25 | 11.3 | 18 | 4.6 | 1.00 |
| $N_2$ | 12.7 | 10 | 13.0 | 16 | 3.6 | 1.00 |
| He | 8 | 4 | 6.3 | 13 | 4.0 | 1.00 |
| He | 12.7 | 4 | 8.5 | 17.5 | 3.5 | 1.00 |

[48] H. S. W. Massey and E. H. S. Burhop, *Electronic and Ionic Impact Phenomena* (Clarendon Press, Oxford, England, 1952), p. 170.

### D. Intensity Ratio of Lines 3 and 4

Figure 15 shows the ratio $I_3/I_4$ of the intensity of line 3 to that of line 4 as a function of pressure for liquid nitrogen cooled and liquid helium cooled hollow cathodes, with two cathode diameters. Two general observations can be made from Fig. 15: At higher pressures the intensity ratio for the smaller diameter cathode is higher than the ratio for the larger diameter cathode; and as the pressure is decreased the ratio tends to increase and then decrease rather sharply.

The first behavior can be understood by the following reasoning: Relative to the initial level $4f\,^2F_{7/2}$ of line 9, the $4s\,^2S_{1/2}$ level has a dynamical population about thirty times its statistical population, while the corresponding ratio for the $4p$ term is only about 2.5. Since at the same pressure the excited ions undergo fewer collisions with helium atoms in the smaller diameter cathode before suffering a de-exciting collision with the electric field or cathode walls, the atoms that do emit have undergone fewer collisions than those in the larger cathode, and thus have more nearly the dynamical distribution. This effect increases the magnitude of $I_3$ more than that of $I_4$, thereby increasing the ratio at the same pressure in the smaller diameter cathode.

The turnover in the $I_3/I_4$ ratio seems to be associated with a change in the rate of excitation for the upper levels of lines 3 and 4. As the low-pressure operating limit is approached, the cathode-anode potential difference, which is nominally constant, increases relatively abruptly and almost certainly changes the electron energy distribution. Since the electron excitation cross sections for $n=4$ can be expected to have maxima near threshold, and it is reasonable to expect the $S$ cross section to have a lower maximum and to decrease more quickly with electron energy than the $P$ cross

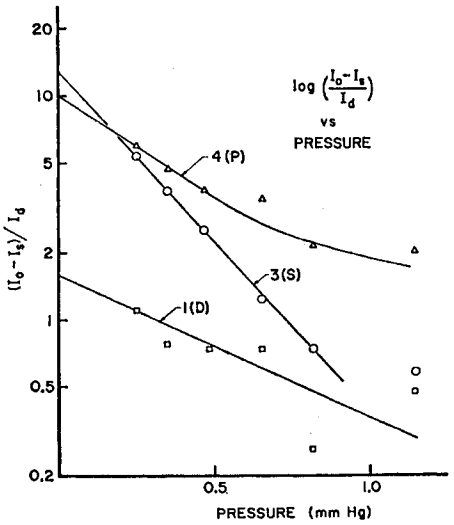


FIG. 14. $\text{Log}(I_o-I_s)/I_d$ versus pressure for several lines of the He II $3s,\ p,\ d-4s,\ p,\ d,^1f$ complex as observed in a liquid nitrogen cooled hollow cathode 12.7 mm in diam. The $l$ value of the upper ($n=4$) level is given in parentheses.

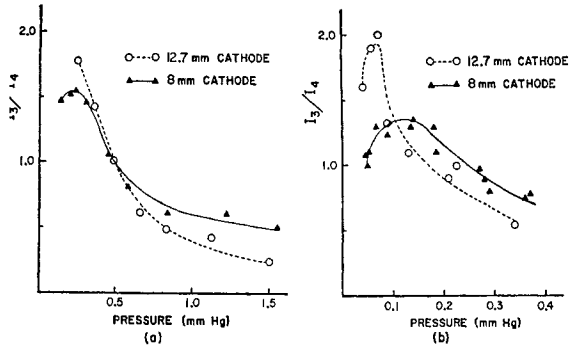


FIG. 15. Ratio $I_3/I_4$ of the intensities of lines 3 and 4 of the He II $3s,\ p,\ d-4s,\ p,\ d,\ f$ complex as a function of pressure for a hollow cathode cooled in (a) liquid nitrogen, (b) liquid helium.

section,[49] the observed turnover can be accounted for by simply assuming that the average electron energy is above a value determined by the exact, and presently unknown, shapes of the cross-section curves, and that it increases as the operating voltage increases; for then, whether one assumes that the excitation is accomplished by the high-energy electrons in the tail of a Boltzmann distribution or by a more or less isolated peak of electrons with energy above threshold, the number of atoms in the $P$ state relative to the number in the $S$ state is increased.

### E. Intensity Variation with Current

No appreciable variation in the relative intensities of the components as a function of current was found in this study. The small variations that were observed are consistent with the tendency of the increased current to increase the temperature in the hollow cathode. Thus, this study does not confirm the observation made by Herzberg[12] that the components tended toward a statistical distribution with increased current as well as with increased pressure. Herzberg's conclusion might have been based on a photographic comparison of the relative intensities of lines 3 and 4: If the increase in current caused an increase in the average electron energy, the effect of the change in the relative rates of excitation which causes line 4 to increase relative to line 3, as noted above, could easily have been misinterpreted as a tendency towards the statistical distribution in which line 4 has a greater intensity than line 3.

### F. Comparison of the Relative Intensities in the Liquid Helium and Liquid Nitrogen Cooled Hollow Cathodes

The principal difference between the measurements using the liquid nitrogen and liquid helium cooled hollow cathodes is that the pressure at which com-

[49] D. G. Hummer (private communication).

parable intensity ratios were observed was very much lower in the liquid He cooled cathode. If it is assumed that the behavior of the relative intensities depends only on the average time between collisions, then it ought to be possible to scale the measurements. It is well known that in a gas, the mean time between collisions is proportional to the square root of the temperature. Taking for the temperatures in the discharge region in the two cases, the temperature determined from the width of the He I $1s2p\ ^3P_0-1s4s\ ^3S_1$ line of the 4713 Å multiplet (100°K for liquid nitrogen and 35°K for liquid helum), one finds that the pressures measured in the liquid helium cooled cathode should be multiplied by a factor of about 1.7 in order to scale them to the conditions in the liquid nitrogen cooled cathode. Using this factor we find general agreement, but not exact coincidence, and conclude that there are other processes, not clearly understood, which must be taken into account.

### G. Summary of Intensity Study

Within the experimental uncertainty the results of the intensity study can be summarized as follows:

So long as the pressure in the discharge region is high enough, the levels are populated according to their statistical distributions.

At low pressures, the population of an excited level depends upon the product of its rate of excitation and its lifetime.

The usual multiplet intensity rules are satisfied.

The excitation function of a level with a specified $n$ depends only on its $l$ value.

There is no mixing between the nearly degenerate states with the same $j$ but different $l$.

The relative rates of excitation for the various levels may change if the average electron energy changes.

To at least a fair approximation, the transition between dynamical and statistical intensities depends only on the average time between collisions.

#### ACKNOWLEDGMENTS

The authors are particularly indebted to R. Chabbal of Laboratoire Aimé Cotton, who designed the instrument used in this study and taught us how to use it, and to O. S. Duffenduck for his helpful advice and his efforts in procuring very good Fabry-Perot flats. We owe thanks to many others: especially to R. N. Dexter and J. R. Dillinger for their advice and cooperation in the use of liquid helium; to J. D. Garcia for his advice on the calculation of the levels; to Linda deNoyer, James Margenau, and Miranda Tung for their help in reducing data and performing calculations; and to Mark Daehler, D. P. McNutt, and D. J. Schroeder for fruitful ideas contributed in discussions of this work.

PHYSICAL REVIEW VOLUME 135, NUMBER 1A 6 JULY 1964

# Primary Ionization Coefficient Measurements in Penning Mixtures

LORNE M. CHANIN AND G. D. RORK
*Honeywell Research Center, Hopkins, Minnesota*
(Received 6 February 1964; revised manuscript received 16 March 1964)

Measurements have been made of the electron ionization coefficient $\eta$ in helium-hydrogen and neon-hydrogen gas mixtures over an extended range of $E/p_0$ values. The present results show a variation of $\eta$ with $E/p_0$ and hydrogen concentration similar to that previously obtained by Kruithof and Penning for the case of neon-argon mixtures. The maximum values of $\eta$ observed of 0.0302 and 0.0285 $V^{-1}$ were obtained for hydrogen concentrations of 0.1% and at $E/p_0$ (V/cm×Torr) values of 15.0 and 3.0 for helium-hydrogen and neon-hydrogen mixtures, respectively. Comparison is made of these results with the neon-argon measurements of Kruithof and Penning. In addition, the present data are compared with ionization measurements obtained using other techniques.

## I. INTRODUCTION

IN a binary gas mixture if the energy of the metastable state of the main constituent exceeds the ionization energy of the minor component, such a mixture is generally referred to as a Penning mixture. One of the most significant characteristics of such a mixture is the enhancement of the ionization coefficient of the resulting mixture over that of either constituent. This property was demonstrated in detail in the measurements of Kruithof and Penning[1] for the case of neon-argon mixtures. In the present investigation measurements were made of the ionization coefficient $\eta$ in helium-hydrogen and neon-hydrogen mixtures. The electron ionization coefficient $\eta$ is defined as the average number of ionizing collisions for each volt potential difference through which an electron has fallen. The present paper describes the results of these measurements and discusses the enhancement of the ionization coefficient for various Penning mixtures.

## II. APPARATUS

The apparatus and technique used in the present studies have been described[2] in detail previously, hence

[1] A. A. Kruithof and F. M. Penning, Physica **6**, 430 (1937).

[2] L. M. Chanin and G. D. Rork, Phys. Rev. **132**, 2547 (1963).

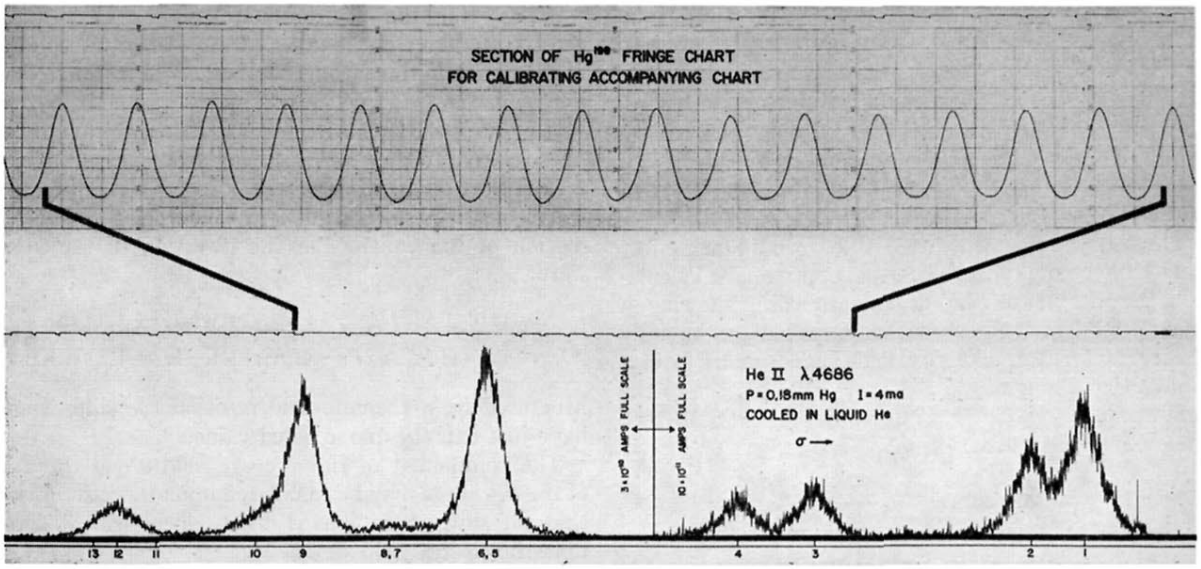


FIG. 6. The He II $3s, p, d-4s, p, d, f$ line complex observed in a liquid helium cooled hollow cathode. The calibration fringe chart is related to the spectrum chart through the coded intercalibration marks at the top of each chart. The heavy lines between the charts indicate the portion of the spectrum to which the reproduced portion of the fringe chart applies.